International Journal of Mass Spectrometry 305 (2011) 95–102

Contents lists available at ScienceDirect

International Journal of Mass Spectrometry

journal homepage: www.elsevier.com/locate/ijms

Top-down high-resolution electron capture dissociation mass spectrometry for comprehensive characterization of post-translational modifications in *Rhesus* monkey cardiac troponin I

Fangmin Xu[a,b,1], Qingge Xu[a,b,1], Xintong Dong[a], Moltu Guy[a], Huseyin Guner[a,b], Timothy A. Hacker[c], Ying Ge[a,b,*]

[a] Human Proteomics Program, School of Medicine and Public Health, University of Wisconsin-Madison, Madison, WI, USA
[b] Department of Physiology, School of Medicine and Public Health, University of Wisconsin-Madison, Madison, WI, USA
[c] Department of Medicine, School of Medicine and Public Health, University of Wisconsin-Madison, Madison, WI, USA

ARTICLE INFO

Article history:
Received 18 May 2010
Received in revised form 29 August 2010
Accepted 7 September 2010
Available online 16 September 2010

Keywords:
Top-down mass spectrometry
Electron capture dissociation
Phosphorylation
Cardiac troponin I
Heart diseases

ABSTRACT

Top-down high-resolution electron capture dissociation (ECD) mass spectrometry (MS) is a powerful approach for comprehensive characterization of large proteins with labile post-translational modifications (PTMs). Phosphorylation of cardiac troponin I (cTnI) is a prominent determinant of cardiac function. Non-human primates (NHPs) are valuable models for biomedical research due to their genetic similarity to humans. To address the emerging need for in-depth understanding of NHP heart models, we have applied top-down high-resolution tandem mass spectrometry in conjugation with immunoaffinity chromatography purification to comprehensively characterize NHP cTnI. Our data revealed that cTnI affinity purified from NHP *Rhesus* monkey hearts was N-terminally acetylated and mono- or bis-phosphorylated. ECD unambiguously identified Ser22/Ser23 as the only basally phosphorylated sites with a phosphorylation order between these two sites (Ser23 phosphorylates prior to Ser22) which is different from those previously reported for mouse and human cTnI. Our study also strongly supports the nonergodic mechanism of ECD since no neutral loss of phosphates was observed in ECD spectra. Taken together, top-down MS with ECD is extremely valuable for studying labile PTMs in large proteins, which adds critical knowledge to our understanding of protein PTM regulations in health and disease.

1. Introduction

A comprehensive sequence characterization of proteins including the post-translational modification (PTM) and sequence variants (i.e. mutants, splicing isoforms) is extremely important for understanding the protein structure, activity, and function [1,2]. Biological mass spectrometry (MS) [3] is the method of choice for protein characterization as it can provide universal information about the protein modification state without *a priori* knowledge [4]. The well-established "bottom-up" MS strategy involves either in-gel or in-solution digestion of proteins prior to MS analysis, which is now routinely used for protein identification and profiling with high throughput and automation [5–10]. Nevertheless such a "bottom-up" approach has intrinsic limitations for characterizing PTMs and sequence variants mainly due to the partial sequence coverage since only a portion the digested peptides are recovered, and the loss of correlations between the modifications on disparate portions of protein [11]. In contrast, top-down MS strategy emerges as an important method for characterizing large proteins (>200 kDa) with complex PTMs and sequence variants [2,12–22]. The top-down MS approach greatly simplifies sample preparation procedures as no proteolytic digestion is required. Instead, intact proteins are analyzed directly, which provides an "birds' eye" view of the protein revealing all possible modifications [23]. Moreover, it provides much higher sequence coverage (up to 100%) since individual modified protein ions can be isolated in the gas phase (inside the mass spectrometer) and fragmented by tandem mass spectrometry (MS/MS), thus allowing a highly reliable mapping of the modification sites [2,21,22,24]. Top-down MS is primarily performed in mass spectrometers with high resolving power such as Fourier transform ion cyclotron (FT-ICR) [25]. FT-ICR is well-known for its ultra high mass resolution, high mass accuracy,

* Corresponding author at: Human Proteomics Program and Department of Physiology, School of Medicine and Public Health, University of Wisconsin-Madison, 1300 University Ave., SMI 130, Madison, WI 53706, USA. Tel.: +1 608 263 9212; fax: +1 608 265 5512.
E-mail address: yge@physiology.wisc.edu (Y. Ge).
[1] These two authors contributed equally to this work.

1387-3806/$ – see front matter © 2010 Elsevier B.V. All rights reserved.
doi:10.1016/j.ijms.2010.09.007

high sensitivity, and multiple MS/MS techniques including collisionally activated dissociation (CAD) [26], infrared multiphoton dissociation (IRMPD) [27], blackbody infrared radiative dissociation (BIRD) [28,29], and the most recently introduced electron capture dissociation (ECD) [30]. ECD cleaves peptide backbone N–Cα bonds leading to ***c*** and ***z**•* fragment ions, which complements with the traditional energetic dissociation methods for comprehensive protein structural characterization [22,24,31,32]. The most important and unique feature of ECD is its nonergodic nature [30,33], which preserves the labile PTMs during MS/MS process. In contrast, neutral phosphate losses are typically observed in the CAD and other energetic dissociation experiments, making it difficult to localize the phosphorylation sites. ECD is also nonselective, which can generate far greater sequence coverage for proteins than that of CAD [14,30]. Hence, top-down MS with ECD is becoming an extremely valuable tool in mapping labile PTMs such as phosphorylation [2,21,34].

As the 'gold standard' biomarker for diagnosis of heart disease, cardiac troponin I (cTnI) and T (cTnT) are the most cardiac-specific and sensitive biomarkers to date [35]. cTnI, cTnT and cardiac Troponin C (cTnC) are the three subunits of cardiac troponin (cTn), the regulatory protein complex of cardiac contraction and relaxation [36]. Phosphorylation of cTnI is a key mechanism in modulating cardiac function [37–39]. cTnI phosphorylation changes Ca^{2+} binding affinity of cTnC that renders the conformational change and thereby alters myofilament Ca^{2+} sensitivity [38]. A disturbed balance between phosphorylation and dephosphorylation of cTnI could contribute causally to cardiac dysfunction in the transition from compensated hypertrophy to heart failure [38,40,41]. Phosphorylation of cTnI is known to be regulated by protein kinase A (PKA) [42], protein kinase C (PKC) [41,43–46], p21-activated kinase (PAK) [47], protein kinase D (PKD) [48], and cyclic GMP-dependent protein kinase (PKG) [38].

Non-human primates (NHPs) models are used to study a broad array of disease pathogenesis, medical treatments and organ transplantation, and are of high value for pre-clinical testing [49–51]. Among those NHPs, *Rhesus* monkey (also named *Rhesus Macaque* or *Macaca mulatta*) is the most common species explored in laboratories for heart disease and transplantation studies [52,53]. Hence, there is an emerging need for in-depth understanding of NHP myofilament proteins such as cTnI and its PTMs, which will help establish a proper NHP heart model.

In this study, we aim to comprehensively characterize cTnI in *Rhesus* monkey heart to examine the correlation of heart models between NHPs and humans. To address this aim, we have employed top-down high-resolution FT-ICR MS combined with immunoaffinity purification to comprehensively characterize NHP cTnI, with a special focus on its phosphorylation state.

2. Material and methods

All chemicals were purchased from Sigma Chemical Co. (St. Louis, MO, USA) unless noted otherwise. Complete protease and phosphatase inhibitor cocktail tablets were purchased from Roche Diagnostics Corporation (Indianapolis, IN, USA). All solutions were prepared in Milli-Q water (Millipore Corporation, Billerica, MA).

2.1. Immunoaffinity purification of NHP cTn

Heart tissue was obtained from left ventricles of *Rhesus* monkey hearts approved by the University of Wisconsin Animal Care and Use Committee. The excised heart tissue was immediately frozen in liquid nitrogen and stored at −80 °C until cTn protein extraction. The entire cTn complex was purified by the immunoaffinity purification method as described previously [21,22]. Briefly, approximately 1.5 g of heart tissue was homogenized in tissue wash buffer (NaH_2PO_4 500 mM, Na_2HPO_4 100 mM, $MgCl_2$ 100 mM, EGTA 100 mM, NaCl 0.1 M, Triton X-100 1%, DTT 5 mM, protease and phosphatase inhibitor cocktail tablet, PMSF 1 mM, leupeptin 2 μg/mL, pH 7.4) using a Polytron electric homogenizer for 1 min on ice. The homogenate was centrifuged at 13,200 rpm (Centrifuge 5415R, Eppendorf, Hamburg, Germany) for 3 min at 4 °C; the supernatant was discarded and the pellet was resuspended 4 times in total 6 mL (1.5 mL × 4) of protein extraction buffer (0.7 M LiCl, 25 mM Tris, 5 mM EGTA, 0.1 mM $CaCl_2$, 5 mM DTT, 1 mM PMSF, 2 μg/mL leupeptin, and 0.75 mg/mL protease and phosphatase inhibitor cocktail, pH 8.0) and protein extraction was performed with agitation on a rotating mixer (Fisher Scientific Inc., Pittsburgh, PA) at 4 °C for 25, 20, 15 and 10 min sequentially. The sample was then centrifuged at 16,000 rpm (Centrifuge 5415R, Eppendorf, Hamburg, Germany) for 5 min to collect the supernatant. The collected supernatant was further centrifuged at 55,000 rpm (Beckman L-55 ultracentrifuge, Beckman Coulter, Fullerton, CA) for 45 min to completely remove the tissue debris before affinity chromatography purification. The supernatant was incubated with 0.25 mL of CNBr-activated Sepharose CL-4B conjugated with 1.25 mg monoclonal cTnI antibody (anti-troponin I monoclonal antibody MF4 and 14G5, Hytest, Finland) for 40 min at 4 °C. After washing the column with 2 mL of extraction buffer, the bound troponin complex was eluted with 100 mM glycine at pH 2 into four 0.4 mL fractions and neutralized immediately with 40 μL of 1 M MOPS (pH 9). The eluted fractions from the affinity columns were analyzed for enriched protein content by 15% SDS-PAGE gels stained with Coomassie Blue. Analytical repeatability and reproducibility were assessed with at least three technical replicates (independent purification experiments) of three biological replicates.

2.2. Top-down ECD MS analysis of NHP cTnI

Immunoaffinity purified NHP cTn complexes were further separated and desalted using an offline reverse phase protein microtrap (Michrom Bioresources Inc., CA), with a three step reverse phase gradient elution method, first with 1% acetic acid in 30:70 methanol/water, then 1% acetic acid in 50:50 methanol/water and last 1% acetic acid in 70:30 methanol/water. Data were acquired using a 7 T linear trap/FT-ICR (LTQ FT Ultra) hybrid mass spectrometer (Thermo Scientific Inc., Bremen, Germany) equipped with an automated chip-based nano-ESI source (Triversa NanoMate, Advion BioSciences, Ithaca, NY) as described previously [2,21]. The spray voltage was 1.2–1.6 kV versus the inlet of the mass spectrometer, resulting in a flow rate of 50–200 nL/min. Ion transmission into the linear trap and subsequently into the FT-ICR cell was automatically optimized for maximum ion signal. The number of accumulated ions for the full scan linear trap (IT), FT-ICR cell (FT), MS^n FT-ICR cell, and ECD were 3×10^4, 1×10^6, 2×10^7, and 3×10^7, respectively. The resolving power of the FT-ICR mass analyzer was typically set at 200,000 at m/z 400 resulting in an acquisition rate of 1 scan/s. For ECD fragmentation, individual charge states of protein molecular ions were first isolated and then fragmented using 1.8–4.0% electron energy with a 45–55 ms duration with no delay. Typically, 1000–3000 transients were averaged to ensure high quality ECD spectra.

2.3. Data analysis

All FT-ICR spectra were processed with Xtract Software (FT programs 2.0.1.0.6.1.4, Xcalibur 2.0.5, Thermo Scientific Inc., Bremen, Germany) using S/N threshold of 1.5 and fit factor of 40% and validated manually. The resulting mass lists were further assigned

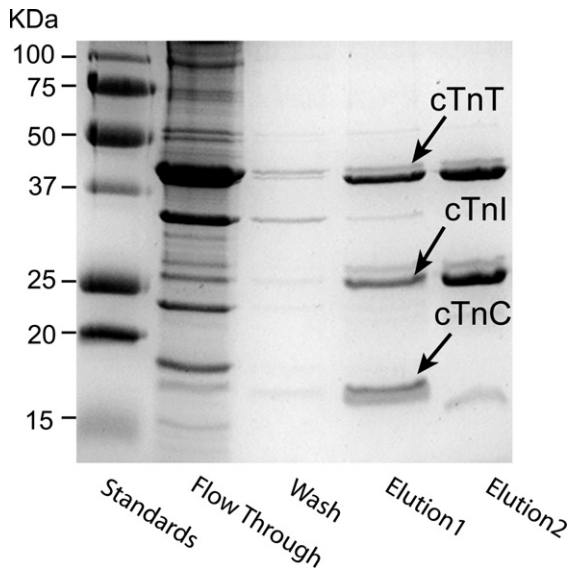

Fig. 1. SDS-PAGE analysis of immunoaffinity purified cTn complexes from *Rhesus* monkey hearts.

using in-house developed "Ion Assignment" software (Version 1.0) based on the protein sequence of *Rhesus* monkey cTnI type3 isoform 1 (NCBI Reference XP_001085820.1) obtained from NCBI protein database. Allowance was made for possible PTMs such as the removal of initial Met, acetylation of the new N-terminus, and variable phosphorylation sites (residues Ser, Thr and Tyr), using a 10 and 20 ppm tolerance for precursor and fragment ions, respectively. The assigned ions were manually validated to ensure the quality of assignments. For fragment ions containing possible phosphorylation sites, the mass of fragment ions were manually examined for 80 Da mass shifts to confirm or exclude the existence of phosphorylation. All reported masses are the most abundant masses. The MS signal intensity values were used to calculate the relative ratios for all the observed protein/fragment ions based on a method developed by Kelleher and co-workers [54] with modifications [2,21,22]. The top five most abundant isotopomer peak heights were integrated to calculate the relative abundance of the intact protein and fragmentation ions.

3. Results

3.1. Immunoaffinity purification and offline separation of NHP cTn

An immunoaffinity purification approach described above was performed to enrich the cTn from the crude myofilament protein extract. Due to tight bindings among cTn complex proteins, the other two cTn components, cTnT and cTnC were eluted along with cTnI during affinity purification although only anti-troponin I monoclonal antibody was used. Typically, the SDS gel displayed three major bands at approximately MW 37, 27 and 18 kDa representing the three subunits of cTn protein complex, cTnT, cTnI and cTnC, respectively (Fig. 1), underscoring the high specificity of the immunoaffinity purification. The three-step reverse phase gradient elution method sufficiently separated the cTn complex into three components, cTnT, cTnI and cTnC, eluted in an order by time. The elution order demonstrated that cTnT was the most hydrophilic protein among those three proteins, whereas cTnC was the most hydrophobic one, consistent with previously reported results [55].

3.2. High-resolution high accuracy MS measurement of NHP cTnI

High-resolution FTMS spectrum of purified cTnI revealed three major ion populations with the most abundant molecular masses of 23858.98, 23938.94 and 24018.91 Da, which were evenly separated with a mass discrepancy of 79.96 Da (Fig. 2). The left peak with a molecular mass of 23858.98 Da was assigned to the reported sequence of *Rhesus* monkey cTnI type 3 isoform 1 which has a calculated molecular mass of 23858.83 Da (Δ = 6.3 ppm) with the removal of initial Met and additional acetylation to the N-terminus. The molecular masses, 23938.94 and 24018.91 Da, were assigned as mono-phosphorylated (Calc'd: 23938.77, Δ = 7.1 ppm) and bis-phosphorylated cTnI (Calc'd: 24018.76, Δ = 6.2 ppm), respectively (Fig. 2), demonstrating the highly accurate molecular weight measurements by FT-ICR MS. No discernible tris-phosphorylation of cTnI was observed, which is estimated to be less than 0.1% of the total cTnI populations in all forms. Only minor proteolytic degradation products were observed because of the stringent control of the heart harvesting and purification procedure that minimizes the influence of *in vitro* proteolytic degradation.

3.3. Mapping phosphorylation sites in NHP cTnI

A single charge state of mono- or bis-phosphorylated precursor ions was isolated individually for ECD. Fig. 3 illustrates the effectiveness of this isolation process, which could almost be considered as "gas-phase purification" of phosphorylated protein ions. Sequentially, the mono- and bis-phosphorylated precursor ions were fragmented by ECD for the localization of phosphorylation sites (Fig. 4). 69 $\boldsymbol{c}$ ions and 70 $\boldsymbol{z}^{\bullet}$ ions were observed in three combined ECD spectra of mono-phosphorylated cTnI (Fig. 4A) and 57 $\boldsymbol{c}$ ions and 70 $\boldsymbol{z}^{\bullet}$ ions were observed in three combined ECD of bis-phosphorylated cTnI (Fig. 4B). A complete coverage of cTnI sequence was achieved by ECD of mono- and bis-phosphorylated cTnI with 13 and 8 $\boldsymbol{c}/\boldsymbol{z}^{\bullet}$ complementary ions, respectively (Fig. 4). All the fragment ions were validated manually to ensure the accuracy in the assignment of phosphorylation sites. In the isolated mono-phosphorylated cTnI ECD spectrum, no phosphorylated product ions were detected for $\boldsymbol{c}_{19}$, $\boldsymbol{c}_{20}$, $\boldsymbol{c}_{21}$ and $\boldsymbol{c}_{22}$ (Fig. 5A1, B1, C1 and D1) as well as other smaller $\boldsymbol{c}$ ions including $\boldsymbol{c}_9$–$\boldsymbol{c}_{18}$. In contrast, mono-phosphorylated $\boldsymbol{c}_{23}$ was observed (Fig. 5E1). This unambiguously identified Ser23 as the first phosphorylation site. No un-phosphorylated $\boldsymbol{c}_{23}$ was detected (estimated to be <1.5% of the mono-phosphorylated $\boldsymbol{c}_{23}$ ions), suggesting full phosphorylation occupancy of Ser23 and no discernable positional isomer for mono-phosphorylated cTnI. Only mono-phosphorylation were observed for $\boldsymbol{c}_{24}$ and the rest of large $\boldsymbol{c}$ ions ($\boldsymbol{c}_{25}$–$\boldsymbol{c}_{208}$) confirmed the phosphorylation site at Ser23 (Fig. 4A). Meanwhile, in the ECD spectrum of isolated bis-phosphorylated cTnI, no phosphorylated product ions were detected for $\boldsymbol{c}_{19}$, $\boldsymbol{c}_{20}$, $\boldsymbol{c}_{21}$ (Fig. 5A2, B2 and C2) as well as other smaller $\boldsymbol{c}$ ions ($\boldsymbol{c}_5$–$\boldsymbol{c}_{18}$) (Fig. 4B) which excluded the possibility of phosphorylation sites present between Ala1 to Ser22. Clearly, mono-phosphorylation was detected for $\boldsymbol{c}_{22}$ ($_p\boldsymbol{c}_{22}$) from ECD of bis-phosphorylated cTnI (Fig. 5D2) which identified Ser22 as an additional phosphorylation site. Only bis-phosphorylation (no un- or mono-phosphorylation) was detected for $\boldsymbol{c}_{23}$ ($_{pp}\boldsymbol{c}_{23}$), $\boldsymbol{c}_{24}$ ($_{pp}\boldsymbol{c}_{24}$) (Fig. 5E2 and F2) and other larger $\boldsymbol{c}$ ions ($\boldsymbol{c}_{25}$–$\boldsymbol{c}_{208}$) (Fig. 4B) suggesting that Ser22 and Ser23 are the only two sites basally phosphorylated in NHP cTnI. Additionally, neither mono- nor bis-phosphorylated $\boldsymbol{z}^{\bullet}$ ions including $\boldsymbol{z}^{\bullet}_4$–$\boldsymbol{z}^{\bullet}_{178}$ ions were observed which confirmed the absence of phophorylation between Glu31 and the C-terminal in NHP cTnI (Fig. 4). The fact that Ser22 was phosphorylated only in bis-phosphorylated cTnI form whereas Ser23 was phosphorylated in both mono- and bis-phosphorylated cTnI forms clearly indicated a phosphorylation

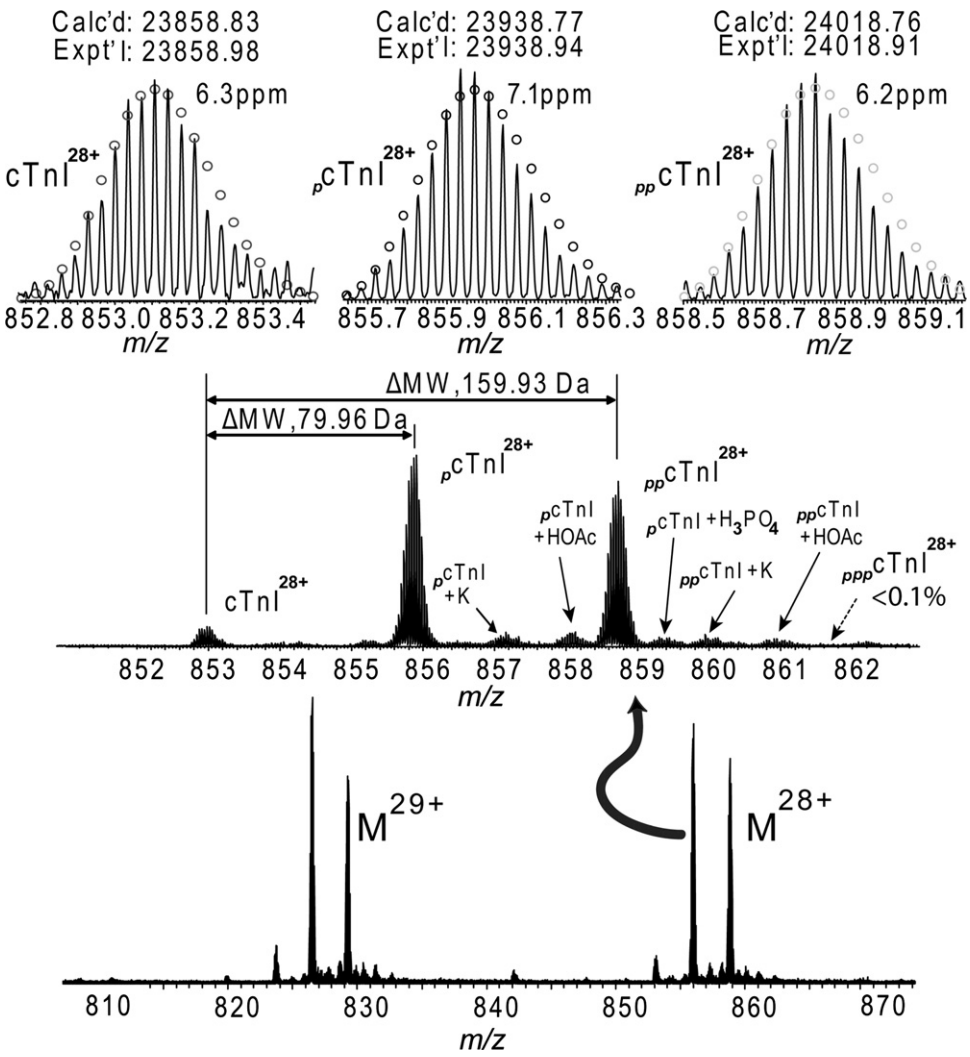

Fig. 2. ESI/FTMS analysis of intact cTnI purified from *Rhesus* monkey hearts. $_{p}$cTnI and $_{pp}$cTnI stand for mono- and bis-phosphorylated cTnI, respectively. ΔMW stands for the molecular weight difference. +K, potassium adduct. +H_3PO_4, non-covalent adduct of phosphoric acid. +HOAc, noncovalent adduct of acetic acid (HOAc). Circles represent the theoretical isotopic abundance distribution of the isotopomer peaks corresponding to the assigned molecular weights. Dashed arrow indicates the expected position of tris-phosphorylated cTnI ($_{ppp}$cTnI) which is not observed here. Calc'd, calculated most abundant molecular weight; Expt'l, experimental most abundant molecular weight.

order between these two phosphorylation sites with Ser23 phosphorylates prior to Ser22.

4. Discussion

4.1. Characterization of endogenous PTMs

This study was aimed to comprehensively characterize the endogenous NHP cTnI including the labile phosphorylation present *in vivo*. Therefore the entire sample preparation procedure was controlled stringently to preserve the endogenous modifications. First, the hearts were harvested immediately following the sacrifice of the animal. The heart tissues were dipped into the liquid nitrogen and stored at −80 °C prior to protein purification. Second, the tissue homogenization/extraction and protein purification was held at low temperature (4 °C) with the inclusion of protease and phosphotase inhibitors to minimize the potential modifications occurring *in vitro*. Third, the samples were acidified with 1% TFA before loading on reverse phase trap for desalting since enzyme activities are known to be reduced significantly in acidic conditions [56]. Fourth, the MS analysis was performed right after separation and desalting procedure. Both SDS-PAGE and MS analyses confirmed that the purification process was controlled very well since only

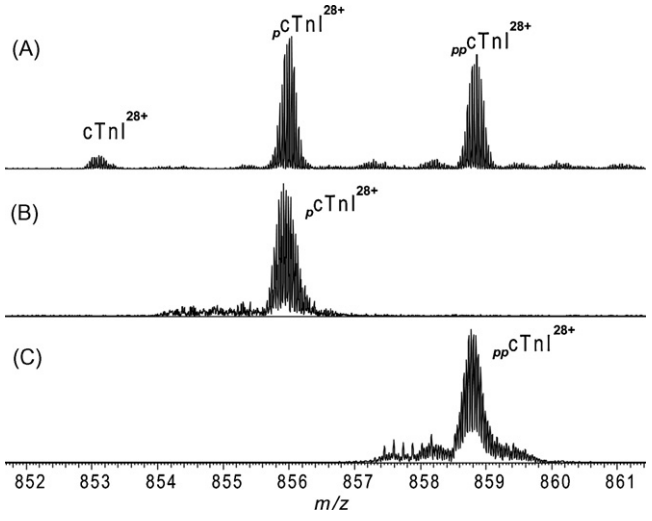

Fig. 3. Isolation of a single charge state (M^{28+}) of *Rhesus* monkey cTnI phosphorylated ions. A, a mixture of un-, mono- and bis-phosphorylated cTnI; B, mono-phosphorylated cTnI; C, bis-phosphorylated cTnI.

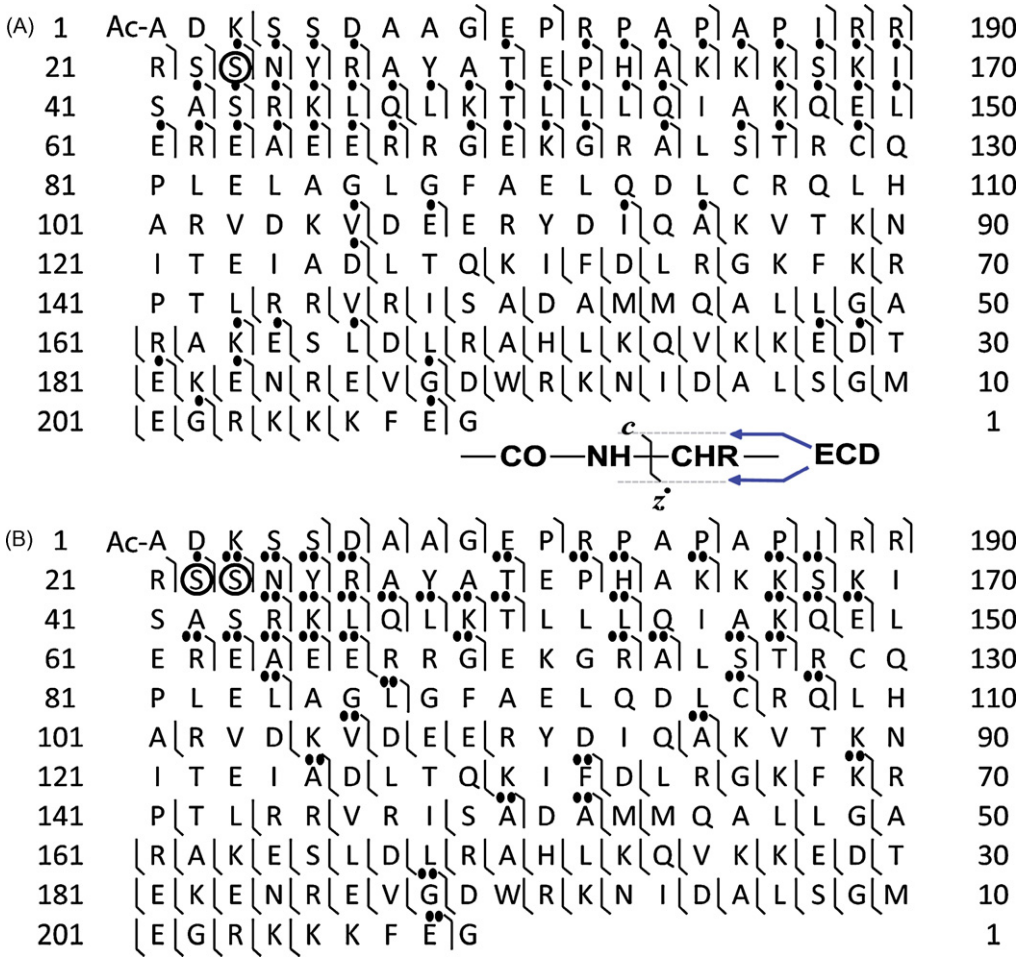

Fig. 4. MS/MS product maps from three ECD spectra of mono- (A) and bis-phosphorylated (B) cTnI, respectively. Fragment assignments were made to the DNA-predicted sequence of *Rhesus* monkey cTnI, type3 (NCBI XP_001085820.1) with the removal of N-terminal Met and acetylation at the new terminus. Single dot, only mono-phosphorylated fragment ion observed; double dots, only bis-phosphorylated fragment ions observed. Identified phosphorylation sites were highlighted in circles.

minor cTn degradation products were found. To verify the repeatability and reproducibility of our experiments, we have analyzed a total of three biological replicates each with 3–5 technical replications. The modification levels in *Rhesus* monkey NHP cTnI including phosphorylation were comparable in three biological replicates and highly reproducible and repeatable. In addition, to address the concern whether the specific antibody epitope could have an effect on the selection of phosphorylation sites or abundance, we have used two different cTnI antibodies with distinct cTnI epitope regions (N-terminal residues 1–23 versus C-terminal residues 190–196 of cTnI), which yielded consistent results for *Rhesus* monkey NHP cTnI phosphorylation without any selective enrichment of certain types of phosphorylated species of cTnI (data not shown). Therefore, the method we established here is reliable for probing the protein modification state in the endogenous proteins present *in vivo*.

4.2. Phosphorylation of NHP cTnI

Here our data unambiguously identified Ser22 and Ser23 as the only phosphorylation sites present in NHP cTnI with a sequential (or ordered) phosphorylation. Phosphorylation of Ser22/23 is mediated by PKA and can be cross-phosphorylated by PKC ($\delta/\beta/\varepsilon$ isozymes) [38–46]. The phosphorylation of Ser22/23 reduces Ca^{2+}-sensitivity of myofilaments and enhances relaxation during increases in after load, which is thought to aid in the relaxation of heart [38,46]. Other phosphorylation sites on cTnI such as Ser43, Ser44 and Thr143 have been shown in other studies and are also substrates of PKC [38,43–46]. The phosphorylation sites on Ser43, Ser44 and Thr143 were identified *in vitro* under high phosphorylation conditions [43–46]. In contrast, the cTnI analyzed here were obtained from healthy, unstressed *Rhesus* monkey NHP hearts *in vivo* so that their phosphorylation state could be different from *in vitro* or in diseased hearts. The potential low levels of other PKC phosphorylation species (<0.1%) could also explain why these phosphorylation sites were not observed or they may be beyond the limits of our method to detect these sites. We believe further development of FT-ICR instruments (hopefully in the near future) and methods will improve sensitivity and detection limits allowing better detection of protein phosphorylations present at very low abundance.

The phosphorylated sites identified *in vivo* in this study (Ser22/23) are consistent with those we reported previously from other species including mouse, swine, and human [19,21,22]. Intriguingly, the phosphorylation order of amino acid residues in the sequence of NHP cTnI is different from the ones in other mammalian species that we reported previously [19,21]. Ser23 was phosphorylated prior to Ser22 in *Rhesus* monkey NHP cTnI whereas phosphorylation of Ser23 occurred after Ser22 in human cTnI. In mouse cTnI, no clear order was revealed since about 60% of mono-phosphorylated cTnI species phosphorylates at Ser22 and 40% at Ser23. A comparison of phosphorylation order in monkey ver-

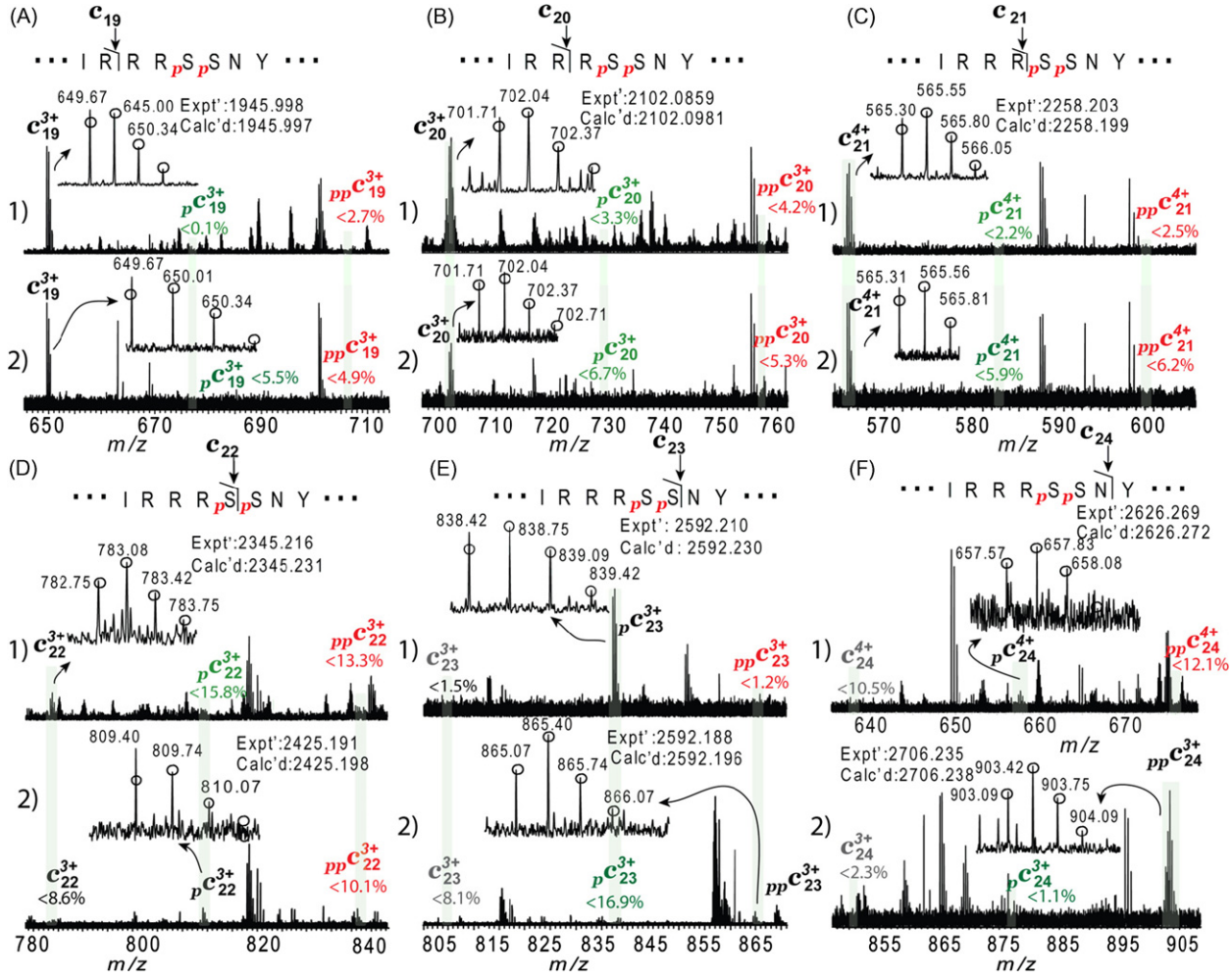

Fig. 5. Key ECD fragment ions for mapping phosphorylation sites of *Rhesus* monkey cTnI. A–F, representative MS/MS spectra of $\boldsymbol{c}_{19}$–$\boldsymbol{c}_{24}$ ions from ECD of mono- (1) and bis-phosphorylated (2) cTnI, respectively. The positively identified isotopomer peak profiles of *c* ions were expanded in each spectrum accordingly. The abbreviated amino acid sequences were listed on the top of each panel (A–F). Circles represent the theoretical isotopic abundance distribution of the isotopomer peaks corresponding to the assigned molecular weights. Calc'd, calculated most abundant molecular weight; Expt'l, experimental most abundant molecular weight.

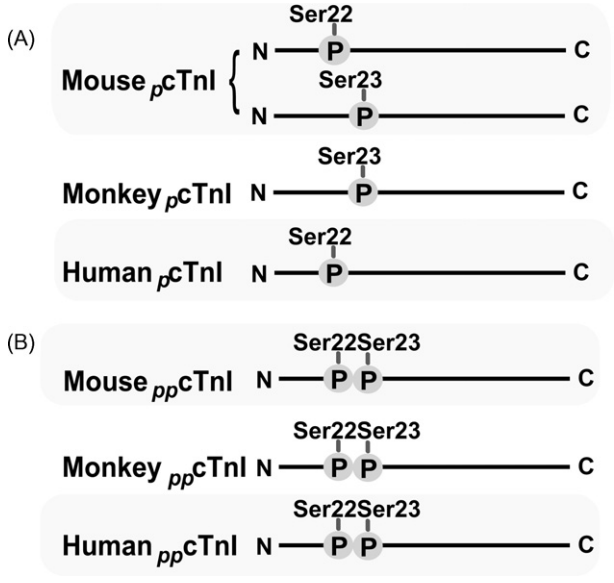

Fig. 6. Comparison of phosphorylation order between Ser22 and Ser23 sites of *Rhesus* monkey versus mouse and human cTnI. (A) Identified phosphorylation site(s) in mono-phosphorylated cTnI ($_p$cTnI), and (B) identified phosphorylation sites in bis-phosphorylated cTnI ($_{pp}$cTnI).

sus mouse and human cTnI is illustrated in Fig. 6. Nevertheless, the potential role of ordered phosphorylation in cTnI is yet to be explored.

5. Conclusion

Here we have employed high-resolution high accuracy FT-ICR MS with ECD for a comprehensive characterization of endogenous cTnI immunoaffinity purified from the left ventricular NHP (*Rhesus* monkey) heart tissue. The entire sample preparation procedure was stringently controlled to preserve the modifications present *in vivo* and minimize the artifactual *in vitro* modifications. Our top-down ECD data unambiguously mapped two basal phosphorylation sites (Ser22 and Ser23) and determined the ordered (or sequential) phosphorylation between these two sites. In contrast to conventional energetic dissociation methods, no neutral loss of phosphate groups were observed in the ECD spectra of isolated individual charge state of intact proteins which strongly supports the nonergodic mechanism of ECD. Thus, we have demonstrated that top-down ECD MS is a powerful method for mapping phosphorylation sites to a single amino acid residue as well as determining the order of multiple phosphorylation sites in large proteins with a potential high impact in biomedical research.

Acknowledgements

This work is dedicated to Professor Catherine Costello for her outstanding achievements in the field of biological mass spectrometry as a 2010 ACS Field and Franklin Awardee. We thank Chad Dooley, Jiang Zhang, Han Zhang, and Matthew Lawrence for assistance with protein purification, data analysis, and helpful discussions. This work was supported by the Wisconsin Partnership Fund for a Healthy Future and American Heart Association Scientist Development Grant 0735443Z (to YG).

References

[1] M. Mann, O.N. Jensen, Proteomic analysis of post-translational modifications, Nat. Biotechnol. 21 (2003) 255–261.
[2] Y. Ge, I.N. Rybakova, Q. Xu, R.L. Moss, Top-down high-resolution mass spectrometry of cardiac myosin binding protein C revealed that truncation alters protein phosphorylation state, Proc. Natl. Acad. Sci. U.S.A. 106 (2009) 12658–12663.
[3] F.W. McLafferty, E.K. Fridriksson, D.M. Horn, M.A. Lewis, R.A. Zubarev, Biochemistry—biomolecule mass spectrometry, Science 284 (1999) 1289–1290.
[4] D. Nedelkov, U.A. Kiernan, E.E. Niederkofler, K.A. Tubbs, R.W. Nelson, Population proteomics—the concept, attributes, and potential for cancer biomarker research, Mol. Cell Proteomics 5 (2006) 1811–1818.
[5] X.M. Han, A. Aslanian, J.R. Yates, Mass spectrometry for proteomics, Curr. Opin. Chem. Biol. 12 (2008) 483–490.
[6] J.R. Yates, Mass spectrometry—from genomics to proteomics, Trends Genet. 16 (2000) 5–8.
[7] S.P. Gygi, R. Aebersold, Mass spectrometry and proteomics, Curr. Opin. Chem. Biol. 4 (2000) 489–494.
[8] M.P. Washburn, D. Wolters, J.R. Yates, Large-scale analysis of the yeast proteome by multidimensional protein identification technology, Nat. Biotechnol. 19 (2001) 242–247.
[9] B. Bogdanov, R.D. Smith, Proteomics by FTICR mass spectrometry: top down and bottom up, Mass Spectrom. Rev. 24 (2005) 168–200.
[10] X. Du, S.J. Callister, N.P. Manes, J.N. Adkins, R.A. Alexandridis, X. Zeng, J.H. Roh, W.E. Smith, T.J. Donohue, S. Kaplan, R.D. Smith, M.S. Lipton, A computational strategy to analyze label-free temporal bottom-up proteomics data, J. Proteome Res. 7 (2008) 2595–2604.
[11] B.T. Chait, Mass Spectrometry: Bottom-up or Top-Down? Science 314 (2006) 65–66.
[12] N.L. Kelleher, H.Y. Lin, G.A. Valaskovic, D.J. Aaserud, E.K. Fridriksson, F.W. McLafferty, Top down versus bottom up protein characterization by tandem high-resolution mass spectrometry, J. Am. Chem. Soc. 121 (1999) 806–812.
[13] N.L. Kelleher, Top-down proteomics, Anal. Chem. 76 (2004) 197A–203A.
[14] Y. Ge, B.G. Lawhorn, M. ElNaggar, E. Strauss, J.H. Park, T.P. Begley, F.W. McLafferty, Top down characterization of larger proteins (45 kDa) by electron capture dissociation mass spectrometry, J. Am. Chem. Soc. 124 (2002) 672–678.
[15] F. Meng, Y. Du, L.M. Miller, S.M. Patrie, D.E. Robinson, N.L. Kelleher, Molecular-level description of proteins from saccharomyces cerevisiae using quadrupole FT hybrid mass spectrometry for top down proteomics, Anal. Chem. 76 (2004) 2852–2858.
[16] X.M. Han, M. Jin, K. Breuker, F.W. McLafferty, Extending top-down mass spectrometry to proteins with masses greater than 200 kilodaltons, Science 314 (2006) 109–112.
[17] V. Zabrouskov, J.P. Whitelegge, Increased coverage in the transmembrane domain with activated-ion electron capture dissociation for top-down Fourier-transform mass spectrometry of integral membrane proteins, J. Proteome Res. 6 (2007) 2205–2210.
[18] J.A. Jebanathirajah, J.L. Pittman, B.A. Thomson, B.A. Budnik, P. Kaur, M. Rape, M. Kirschner, C.E. Costello, P.B. O'Connor, Characterization of a new qQq-FTICR mass spectrometer for post-translational modification analysis and top-down tandem mass Spectrometry of whole proteins, J. Am. Soc. Mass Spectrom. 16 (2005) 1985–1999.
[19] V. Zabrouskov, Y. Ge, J. Schwartz, J.W. Walker, Unraveling molecular complexity of phosphorylated human cardiac troponin I by top down electron capture dissociation/electron transfer dissociation mass spectrometry, Mol. Cell Proteomics 7 (2008) 1838–1849.
[20] R. Sancho Solis, Y. Ge, J.W. Walker, Single amino acid sequence polymorphisms in rat cardiac troponin revealed by top-down tandem mass spectrometry, J. Muscle Res. Cell Motil. 29 (2008) 203–212.
[21] S. Ayaz-Guner, J. Zhang, L. Li, J.W. Walker, Y. Ge, In vivo phosphorylation site mapping in mouse cardiac troponin I by high resolution top-down electron capture dissociation mass spectrometry: Ser22/23 are the only sites basally phosphorylated, Biochemistry 48 (2009) 8161–8170.
[22] J. Zhang, X. Dong, T.A. Hacker, Y. Ge, Deciphering modifications in swine cardiac troponin I by top-down high-resolution tandem mass spectrometry, J. Am. Soc. Mass Spectrom. 21 (2010) 940–948.
[23] N. Siuti, N.L. Kelleher, Decoding protein modifications using top-down mass spectrometry, Nat. Methods 4 (2007) 817–821.
[24] P. Kuhn, Q.G. Xu, E. Cline, D. Zhang, Y. Ge, W. Xu, Delineating Anopheles gambiae coactivator associated arginine methyltransferase 1 automethylation using top-down high resolution tandem mass spectrometry, Protein Sci. 18 (2009) 1272–1280.
[25] A.G. Marshall, C.L. Hendrickson, G.S. Jackson, Fourier transform ion cyclotron resonance mass spectrometry: a primer, Mass Spectrom. Rev. 17 (1998) 1–35.
[26] M.W. Senko, J.P. Speir, F.W. McLafferty, Collisional activation of large multiply-charged ions using Fourier-transform mass-spectrometry, Anal. Chem. 66 (1994) 2801–2808.
[27] D.P. Little, J.P. Speir, M.W. Senko, P.B. Oconnor, F.W. McLafferty, Infrared multiphoton dissociation of large multiply-charged ions for biomolecule sequencing, Anal. Chem. 66 (1994) 2809–2815.
[28] W.D. Price, P.D. Schnier, E.R. Williams, Tandem mass spectrometry of large biomolecule ions by blackbody infrared radiative dissociation, Anal. Chem. 68 (1996) 859–866.
[29] Y. Ge, D.M. Horn, F.W. McLafferty, Blackbody infrared radiative dissociation of larger (42 kDa) multiply charged proteins, Intl. J. Mass Spectrom. 210 (2001) 203–214.
[30] R.A. Zubarev, D.M. Horn, E.K. Fridriksson, N.L. Kelleher, N.A. Kruger, M.A. Lewis, B.K. Carpenter, F.W. McLafferty, Electron capture dissociation for structural characterization of multiply charged protein cations, Anal. Chem. 72 (2000) 563–573.
[31] N.A. Kruger, R.A. Zubarev, B.K. Carpenter, N.L. Kelleher, D.M. Horn, F.W. McLafferty, Electron capture versus energetic dissociation of protein ions, Intl. J. Mass Spectrom. 182 (1999) 1–5.
[32] C. Zhao, B. Xie, S.Y. Chan, C.E. Costello, P.B. O'Connor, Collisionally activated dissociation and electron capture dissociation provide complementary structural information for branched permethylated oligosaccharides, J. Am. Soc. Mass Spectrom. 19 (2008) 138–150.
[33] R.A. Zubarev, N.L. Kelleher, F.W. McLafferty, Electron capture dissociation of multiply charged protein cations. A nonergodic process, J. Am. Chem. Soc. 120 (1998) 3265–3266.
[34] S.D.H. Shi, M.E. Hemling, S.A. Carr, D.M. Horn, I. Lindh, F.W. McLafferty, Phosphopeptide/phosphoprotein mapping by electron capture dissociation mass spectrometry, Anal. Chem. 73 (2001) 19–22.
[35] L. Babuin, A.S. Jaffe, Troponin: the biomarker of choice for the detection of cardiac injury, CMAJ 173 (2005) 1191–1202.
[36] S. Takeda, A. Yamashita, K. Maeda, Y. Maeda, Structure of the core domain of human cardiac troponin in the Ca(2+)-saturated form, Nature 424 (2003) 35–41.
[37] R.J. Solaro, P. Rosevear, T. Kobayashi, The unique functions of cardiac troponin I in the control of cardiac muscle contraction and relaxation, Biochem. Biophys. Res. Commun. 369 (2008) 82–87.
[38] J. Layland, R.J. Solaro, A.M. Shah, Regulation of cardiac contractile function by troponin I phosphorylation, Cardiovasc. Res. 66 (2005) 12–21.
[39] M.P. Sumandea, E.M. Burkart, T. Kobayashi, P.P. De Tombe, R.J. Solaro, Molecular and integrated biology of thin filament protein phosphorylation in heart muscle, Ann. N. Y. Acad. Sci. 1015 (2004) 39–52.
[40] J. van der Velden, Z. Papp, R. Zaremba, N.M. Boontje, J.W. de Jong, V.J. Owen, P.B. Burton, P. Goldmann, K. Jaquet, G.J. Stienen, Increased Ca^{2+}-sensitivity of the contractile apparatus in end-stage human heart failure results from altered phosphorylation of contractile proteins, Cardiovasc. Res. 57 (2003) 37–47.
[41] S.B. Scruggs, L.A. Walker, T. Lyu, D.L. Geenen, R.J. Solaro, P.M. Buttrick, P.H. Goldspink, Partial replacement of cardiac troponin I with a non-phosphorylatable mutant at serines 43/45 attenuates the contractile dysfunction associated with PKCepsilon phosphorylation, J. Mol. Cell Cardiol. 40 (2006) 465–473.
[42] R.J. Solaro, A.J.G. Moir, S.V. Perry, Phosphorylation of troponin-I and inotropic effect of adrenaline in perfused rabbit heart, Nature 262 (1976) 615–617.
[43] T.A. Noland, R.L. Raynor, J.F. Kuo, Identification of sites phosphorylated in bovine cardiac troponin-I and troponin-T by protein kinase-C and comparative substrate activity of synthetic peptides containing the phosphorylation sites, J. Biol. Chem. 264 (1989) 20778–20785.
[44] N.M. Jideama, T.A. Noland Jr., R.L. Raynor, G.C. Blobe, D. Fabbro, M.G. Kazanietz, P.M. Blumberg, Y.A. Hannun, J.F. Kuo, Phosphorylation specificities of protein kinase C isozymes for bovine cardiac troponin I and troponin T and sites within these proteins and regulation of myofilament properties, J. Biol. Chem. 271 (1996) 23277–23283.
[45] Y.Q. Pi, K.R. Kemnitz, D.H. Zhang, E.G. Kranias, J.W. Walker, Phosphorylation of troponin I controls cardiac twitch dynamics—evidence from phosphorylation site mutants expressed on a troponin I-null background in mice, Circ. Res. 90 (2002) 649–656.
[46] T. Kobayashi, R.J. Solaro, Calcium, thin filaments, and the integrative biology of cardiac contractility, Ann. Rev. Physiol. 67 (2005) 39–67.
[47] N. Buscemi, D.B. Foster, I. Neverova, J.E. Van Eyk, p21-activated kinase increases the calcium sensitivity of rat triton-skinned cardiac muscle fiber bundles via a mechanism potentially involving novel phosphorylation of troponin I, Circ. Res. 91 (2002) 509–516.
[48] R.S. Haworth, F. Cuello, T.J. Herron, G. Franzen, J.C. Kentish, M. Gautel, M. Avkiran, Protein kinase D is a novel mediator of cardiac troponin I phosphorylation and regulates myofilament function, Circ. Res. 95 (2004) 1091–1099.
[49] A.H. Nagahara, T. Bernot, M.H. Tuszynski, Age-related cognitive deficits in *Rhesus Macaques* mirror human deficits on an automated test battery, Neurobiol. Aging 31 (2008) 1020–1031.
[50] J. Toelen, J. Deprest, A ray of light for fetal therapy, Hum. Gene Ther. 21 (2010) 137–139.

[51] D.T. Pals, J. Orley, A non-human primate model for evaluating the potential of antential of antihypertensive drugs to cause orthostatic hypotension, J. Pharmacol. Methods 9 (1983) 183–192.
[52] H. Huang, H. Tang, D.G. Yan, Y. Zhang, J. Li, L. Wang, Evaluation of cardiac function in high rate paced *Macaca mulatta*, Int. J. Cardiol. 125 (2008)S55.
[53] C.M. Porter, J.A. Horvath-Arcidiacono, A.K. Singh, K.A. Horvath, E.T. Bloom, M.M. Mohiuddin, Characterization and expansion of baboon CD4(+)CD25(+) Treg cells for potential use in a non-human primate xenotransplantation model, Xenotransplantation 14 (2007) 298–308.
[54] J.J. Pesavento, C.A. Mizzen, N.L. Kelleher, Quantitative analysis of modified proteins and their positional isomers by tandem mass spectrometry: human histone H4, Anal. Chem. 78 (2006) 4271–4280.
[55] D.M. Bunk, M.J. Welch, Characterization of a new certified reference material for human Cardiac Troponin I, Clin. Chem. 52 (2006) 212–219.
[56] I. Neverova, J.E. Van Eyk, Application of reversed phase high performance liquid chromatography for subproteomic analysis of cardiac muscle, Proteomics 2 (2002) 22–31.